Sulkes, M., Lewis, A., Lemley, A., & Cookingham, R. (1976) *Proc. Natl. Acad. Sci. U.S.A. 73*, 4266.

Suzuki, H., & Mizuhashi, S. (1964) *J. Phys. Soc. Jpn. 19*, 724.

Suzuki, T., Uji, K., & Kito, Y. (1976) *Biochim. Biophys. Acta 428*, 321.

Tang, J., & Albrecht, A. C. (1970) in *Raman Spectroscopy*, (Szymanski, H., Ed.) Vol. 2, pp 33-67, Plenum Press, New York, N.Y.

Tokunoga, T., Schichida, Y., & Yoshizawa, T. (1975) *FEBS Lett. 55*, 229.

Tokunaga, F., Govindjee, R., Ebrey, T. G., & Crouch, R. (1977) *Biophys. J. 19*, 191.

Warshel, A. (1977) *Annu. Rev. Biophys. Bioeng. 6*, 273.

Warshel, A., & Karplus, M. (1974) *Calculation of the Resonance Raman Intensities of Schiff Bases of Retinal*, preprint.

Yoshizawa, T., & Wald, G. (1963) *Nature (London) 197*, 1279.

Yoshizawa, T., & Wald, G. (1964) *Nature (London) 201*, 340.

Resonance Raman Spectroscopy of the Retinylidene Chromophore in Bacteriorhodopsin (bR_{570}), bR_{560}, M_{412}, and Other Intermediates: Structural Conclusions Based on Kinetics, Analogues, Models, and Isotopically Labeled Membranes†

Michael A. Marcus‡ and Aaron Lewis*

ABSTRACT: Resonance Raman spectra of various intermediates in the bacteriorhodopsin proton pumping cycle have been obtained at physiological and low temperatures. To interpret these data, spectra of model compounds, bacteriorhodopsin analogues, and isotopically labeled membranes have been measured. These results demonstrate that a protein group interacts with the Schiff base proton and, thus, the chromophore in protonated bacteriorhodopsin species is not a simple protonated Schiff base. This accounts for the abnormally low frequency of the $C{=}N^+H$ vibrational mode in bacteriorhodopsin and other failures to model the chromophore in bR_{570} with a simple butylamine protonated Schiff base of *all-trans*-retinal. To obtain the resonance Raman spectrum of M_{412} at physiological pH and temperatures, a dual beam kinetic technique was developed. We demonstrate that in the fingerprint region of the resonance Raman spectrum M_{412} is modeled accurately by a simple unprotonated butylamine Schiff base of *all-trans*-retinal. Spectral resolution and the solution environment of the membrane suspensions play important roles in this conclusion. Kinetic resonance Raman techniques are also used to monitor the time evolution of the M_{412} species and the intermediates which precede it. We find spectral features in our kinetic data which can be assigned to L_{550}, and we present evidence for a new unprotonated species (X) which occurs before M_{412}. Single pass flow resonance Raman spectra of bR_{560} also have been obtained, and, although bR_{570} and M_{412} appear to have all-trans chromophores, there are 13-cis-like features in the spectra of bR_{560}, L_{550}, and X.

Bacteriorhodopsin, the recently discovered pigment in the purple membrane of *Halobacteri n halobium* (Oesterhelt & Stoeckenius, 1971), has already d a significant impact on the fields of bioenergetics, act transport through membranes, and visual excitation. It nas been demonstrated that this rhodopsin-like pigment acts as a light-driven proton pump (Oesterhelt & Stoeckenius, 1973; Racker & Stoeckenius, 1974; Danon & Stoeckenius, 1974), and one of the functions of the H^+ gradient generated is to act as a driving force for ATP synthesis (Danon & Stoeckenius, 1974; Racker & Stoeckenius, 1974) in agreement with the Mitchell hypothesis (Mitchell, 1961, 1966). Thus, the molecular mechanism of active transport in this energy transducer is of considerable interest.

Resonance Raman spectroscopy is a technique which is capable of yielding important molecular information on the proton pumping function of this membrane-bound protein since it is environmentally and structurally sensitive to the conformation of chromophores in proteins (Lewis & Spoonhower, 1974). In fact, the application of this technique to bacteriorhodopsin has already yielded important structural (Mendelsohn, 1973, 1976; Lewis et al., 1974; Mendelsohn et al., 1974; Aton et al., 1977) and dynamic (Marcus & Lewis, 1977; Campion et al., 1977) information on this protein's active site.

In an early investigation (Lewis et al., 1974), we realized that bacteriorhodopsin, like rhodopsins in visual photoreceptors, undergoes light-induced conformational transformations which are thermally driven subsequent to the photochemical event. Therefore, low temperature techniques were utilized in this study (Lewis et al., 1974) to control the conformational states (intermediates) of the system. From these experiments we were able to show that, although bacteriorhodopsin (bR_{570}) is protonated and can be deuterated, M_{412}, the intermediate preceding the formation of the proton gradient, is unprotonated. The above data suggested that light absorption by the chromophore induces proton movements which are an essential part of this rhodopsin-like system. Furthermore, this investigation indicated that the chromophore was involved not only

† From the School of Applied and Engineering Physics, Cornell University, Ithaca, New York 14853. *Received February 22, 1978; revised manuscript received June 28, 1978.* This work was supported by National Institutes of Health Grant No. EY01377 and starter grants from the Research Corporation and the Petroleum Research Fund, administered by the American Chemical Society. N.A.M. was a National Institutes of Health predoctoral fellow. A.L. was an Alfred P. Sloan Fellow.

‡ Present address: Kodak Research Laboratories, Physics Division, B-81, Kodak Park, Rochester, New York 14650.

0006-2960/78/0417-4722$01.00/0

in the primary photochemical event but also in the subsequent transformations which establish a proton gradient across the cell membrane.

In this paper we present resonance Raman spectra of bR_{570}, bR_{560}, and M_{412} and other intermediates in the proton pumping cycle. Structural conclusions are made for these species based on model compounds, bacteriorhodopsin analogues, and isotopically labeled membranes. Spectral assignments were aided by the theoretical and experimental development of single and dual beam kinetic flow techniques and their comparison with variable temperature steady-state spectra. These investigations have yielded important information on the conformation of the chromophore in the above mentioned bacteriorhodopsin species and have demonstrated that in certain states there exist secondary protein–Schiff base interactions which may be of considerable significance in proton pumping.

Theoretical Considerations

The Photochemical Cycle. The photochemical cycle of light-adapted bacteriorhodopsin has been investigated by various workers (Stoeckenius & Lozier, 1974; Lozier et al., 1975; Kung et al., 1975; Chance et al., 1975; Dencher & Wilms, 1975; Kaufmann et al., 1976; Ippen et al., 1978; Stoeckenius et al., 1977) using transient absorption spectroscopy. Their data and conclusions are summarized below. When visible light impinges upon bacteriorhodopsin (bR_{570}) there is a red shift in the absorbance to 610 nm which occurs in 1.0 ± 0.5 ps at room temperature (Kaufmann et al., 1976; Lewis et al., 1977; Ippen et al., 1978). This red-shifted species has been named bathobacteriorhodopsin (K_{610}) and is stable at liquid nitrogen temperatures (Lozier et al., 1975). It has also been found that K_{610} can be reconverted to bR_{570} by light. Other workers (Goldschmidt et al., 1976) have determined the ratio of quantum yields of the forward ($\phi_{R\rightarrow K}$) and reverse ($\phi_{K\rightarrow R}$) light-driven reactions and have found $\phi_{R\rightarrow K}/\phi_{K\rightarrow R} \approx 0.4$. They have argued that $\phi_{R\rightarrow K} \approx 0.28$ and $\phi_{K\rightarrow R} \approx 0.72$. More recently the same quantum yields were measured directly (Goldschmidt et al., 1977; Becher & Ebrey, 1977), and we use these data in the theoretical calculations presented in this work. All further intermediates in bacteriorhodopsin's photochemical cycle occur thermally in the dark (Lozier et al., 1975). At room temperature bathobacteriorhodopsin decays in about 2 μs to an intermediate absorbing maximally at about 550 nm (Lozier et al., 1975). We call this species L_{550} and it is thought to decay to an unprotonated species M_{412}, discussed above, in about 40 μs. M_{412} is stable for about 5 ms, and recently Becher & Ebrey (1977) have demonstrated that M_{412} has a photoreversible reaction to bR_{570}. There are at least two intermediates (N_{520} and O_{660}) between the decay of M_{412} and the reformation of bR_{570} which occurs in about 10 ms at room temperature.

In addition to this "light-adapted" bR_{570} proton pumping cycle bacteriorhodopsin in the dark reverts with a half-time of 21 min at 20 °C to a species called bR_{560} absorbing maximally at 560 nm. Upon photon absorption bR_{560} is converted to bR_{570} and recently the quantum yield of light-adaptation has been determined by two different groups. Kalisky et al. (1977) and Korenstein & Hess (1977) have measured this quantum yield of light adaptation ($\phi_{D\rightarrow L}$) to be 0.035 ± 0.07 and 0.08 ± 0.02, respectively.

Single Beam Kinetic Spectroscopy. Our previous application of kinetic resonance Raman spectroscopy (KiRRS) to this system of photochemically produced intermediates was based on a variable speed flow method which altered the average concentration of species in the laser beam in a controlled

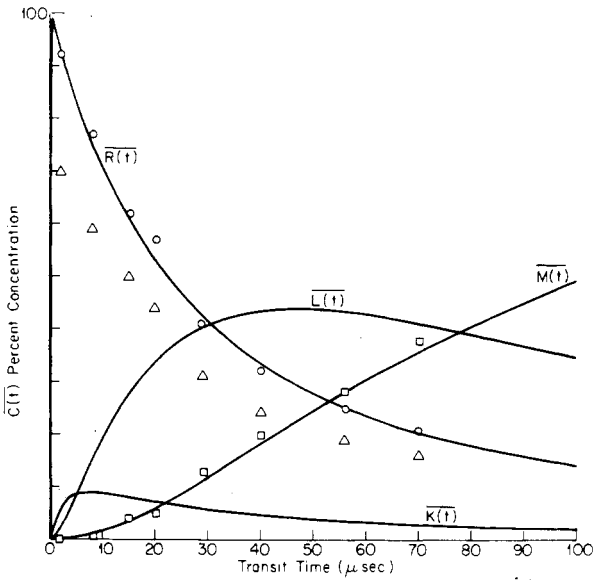

FIGURE 1: Theoretical curves of average concentration of photochemical species ($\overline{C(t)}$) vs. transit time in a 30-mW 457.9-nm laser beam focused to 23 μm. Also shown are experimentally determined average concentration data with □ representing concentrations of M_{412} determined by normalization to the M_{412} resonance Raman spectrum. (△) bR_{570} concentrations using the same normalization as for □. (○) The bR_{570} concentrations normalized to the bR_{570} spectrum.

manner (Marcus & Lewis, 1977). For a system with multiple photolabile species, the number of detected counts (S) at the photomultiplier for a given scattered frequency (ν) is given by the general expression

$$S(\nu) = \sum_i E(\nu)\sigma_{Ri}(\nu) \int_V I(\vec{r})C_i(\vec{r})\mathrm{d}V \qquad (1)$$

where $E(\nu)$ is the overall detection efficiency of the Raman apparatus at frequency ν, σ_{Ri} is the resonance Raman cross-section (cm^2/molecule) of the ith species, $I(\vec{r})$ is the incident laser light intensity, and $C_i(\vec{r})$ is the concentration (molecules/cm^2) of the ith species. This is a generalization of the equation obtained by Mathies et al. (1976) and Callender et al. (1976) for a single photolabile species. In order to effectively utilize eq 1, it is convenient to determine the average concentration $\overline{C_i(R)}$ of the species i in the laser beam. In a flowing sample with uniform or turbulent flow and neglecting depth effects on laser intensity (justified in dilute solutions of effective OD < 0.1), the average concentration $\overline{C_i(\vec{r})}$ of species i is given by

$$\overline{C_i(\vec{r})} = \overline{C_i(t_f - t_i)} = \int_{t_i}^{t_f = 2r_0/V_B + t_i} \frac{C_i(t)\mathrm{d}t}{t_f - t_i} \qquad (2)$$

where r_0 is the laser beam radius, V_B is the bulk flow velocity, and $t_f - t_i$ is the transit time through the laser beam.

In the case of a single beam experiment, t_i is taken to be zero and the observed Raman scattering for the bacteriorhodopsin system with transit times ($t_f < 100$ μs) in the laser beam becomes

$$S(\nu,t_f) = E(\nu)I_0[\sigma_R(\nu)\overline{R(t_f)} + \sigma_K(\nu)\overline{K(t_f)} + \sigma_L(\nu)\overline{L(t_f)} + \sigma_M(\nu)\overline{M(t_f)}] \qquad (3)$$

where $\overline{R(t_f)}$ is the average concentration of bR_{570} and $\overline{K(t_f)}$, $\overline{L(t_f)}$, and $\overline{M(t_f)}$ are the average concentrations of K_{610}, L_{550}, and M_{412}, respectively. Theoretical curves for average concentration vs. transit time in the laser beam are plotted (solid lines) in Figure 1 for 30 mW of 457.9-nm excitation focused to a 23-μm beam diameter. It is seen that, by varying the sample transit time through the laser beam, we vary the av-

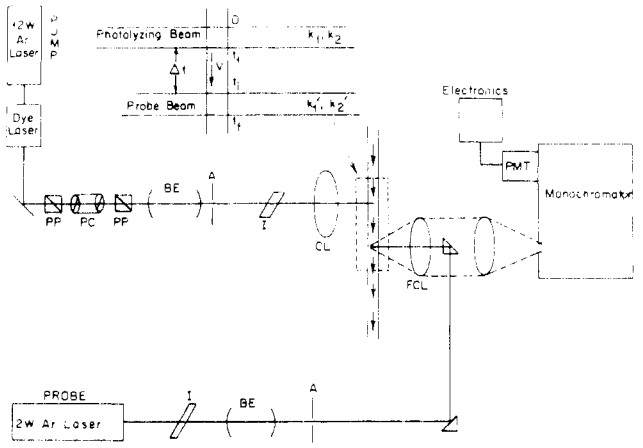

FIGURE 2: Schematic of the dual laser beam apparatus utilized in our experiments. The sample flows vertically as indicated by the vertical arrows. The inset establishes the relationship of some of the symbols which are used in the theoretical considerations section. The photolyzing beam pumps the photochemistry, and the probe beam is utilized to obtain a resonance enhanced Raman spectrum of some intermediate with an optimal concentration corresponding to Δt (inset). All other symbols are as described in the text.

erage composition of the species detected. Thus, when different species have different characteristic vibrational frequencies (as is the case in bacteriorhodopsin), we can monitor the kinetics by observing changes in Raman intensities as a function of sample transit time in the laser beam.

Dual Beam Kinetic Spectroscopy. In some of the experiments, we utilized a dual laser beam technique with the two beams spatially separated as indicated in Figure 2. In this manner it is possible to maximize the extent of photochemistry occurring in the sample with a photolyzing pump beam and to observe Raman spectra of photochemical intermediates with a probe beam.

Figure 2 (inset) shows the flowing sample with two parallel laser beams incident upon it and establishes the relationship of the various symbols in the equations below. In the region between the two laser beams, the light-dependent rate constants for the conversion of bR_{570} to K_{610} and vice versa, k_1 and k_2, respectively, are both zero. Thus the concentration of bR_{570} when it enters the probe beam is the same as its concentration upon leaving the pump beam. If it is experimentally possible to make $R(t_1)$ (concentration of bR_{570} at t_1) shown in Figure 2 (inset) equal to zero then expressions for $L(t)$ and $M(t)$ for $t_1 \leq t \leq t_i$ (where no laser beam is present) become

$$L(t) = L(t_1)e^{-k_4(t-t_1)}$$
$$M(t) = 1 - L(t_1)e^{-k_4(t-t_1)} \quad (4)$$

where k_4 is the rate constant for the formation of M_{412}. It can be shown that, after excitation for ca. 35 μs with a 300-mW laser beam at 573.0 nm focused to 100 μm with a cylindrical lens, the concentrations of bR_{570} and K_{610} are effectively zero. Thus, it is possible to observe an almost pure resonance Raman spectrum of the M_{412} intermediate if (1) we probe downstream far enough so that the exponential factor of eq 4 approaches zero [certainly 1 ms downstream is sufficient (unpublished calculation)] and (2) we control the frequency of the probe beam and the volume it illuminates to minimize multiple hits on molecules which might have been photoconverted from M_{412} to bR_{570} by probe beam induced photon absorption.

Materials and Methods

Experimental Arrangement. A schematic of the dual laser beam apparatus for obtaining photochemical kinetic intermediate resonance Raman data is shown in Figure 2. A Coherent Radiation 12-W argon ion laser was used to pump a Coherent Radiation Model 490 rhodamine 6G dye laser. The frequency of this pump beam was 570–580 nm depending upon the experiment. The probe beam came from a 2-W Coherent Radiation argon ion laser or a Model 52 krypton laser. The laser beams were made nearly uniform by passing them through 10× beam expanders (BE) and then through 1-mm apertures (A). It was found that the laser beams were uniform to within 5% at the sample. Interference filters (I) were used in both beams to block out laser emission lines and dye laser fluorescence. The probe beam was incident in a backscattering arrangement. In some experiments the focusing–collection lens (FCL) was cylindrical to ensure a uniform line image on the sample. This allows direct correlation of the experimental data with the theoretically calculated curves such as those shown in Figure 1 since these calculations assumed that the laser beam was a uniform line image on the sample. In all cases the pump beam was focused on the sample with a 50-mm focal length cylindrical lens (CL) for the reason cited above and to ensure illumination of the entire sample volume in all dual beam experiments. For some experiments a Pockels cell (PC) was inserted between two Glan-Thomson polarizing prisms (PP). By switching the half-wave voltage through the Pockels cell on and off, the pump beam could be effectively switched on and off. In this manner a single beam and double beam experiment could be performed simultaneously, and the data subsequently separated by computer. The monochromator would be stepped only after data were obtained in two channels, one with and the other without the pump beam present. This is possible since the thermal relaxation time of bacteriorhodopsin molecules activated by the pump beam is on the order of ms, whereas the time per channel is 5–10 s.

Spectra were taken with a Spex 1401 double monochromator, equipped with a thermoelectrically cooled RCA C31034 photomultiplier tube (PMT) and home-built photon counting electronics. Data were stored on paper tape via a single channel scaler designed in our laboratory (Perreault et al., 1976) and later analyzed and plotted with a Modcomp II computer. All spectra were taken with 1 or 2 cm^{-1} steps with a counting time of 5–10 s per channel and with the spectrometer slits set for 1–3 cm^{-1} resolution.

Laser beam diameters were measured by translating a razor blade attached to a differential micrometer across the laser beam at its focus. A phototransistor was used as a detector to measure transmitted light. In this manner the profile of the laser beam could be determined. For 457.9-nm laser light the diameter of the focused spot from the probe beam was 23 ± 2 μm, whereas for a 530.9 nm beam it was measured to be 27 ± 2 μm. The diameter of the pump beam focal region was 50 ± 4 μm or 100 ± 5 μm at 570 nm depending on the cylindrical lens utilized. The distance between the two laser beams was measured in a similar fashion.

Polarization measurements were performed with the fixed analyzer method of Proffitt & Porto (1973). A Pockels cell arrangement was utilized to vary the laser polarization by switching on and off the quarter wave voltage to the Pockels cell. Low temperature spectra were obtained with a home built liquid nitrogen immersion cryostat (Spoonhower, 1976).

In order to verify the composition of the flowing samples utilized in our experiments absorption spectra were obtained under identical conditions as the Raman experiments. For the bR_{570} single beam experiments, we estimate that the sample was at least 95% bR_{570}, and for the double beam M_{412} experiments the sample contained a minimum of 85% M_{412}. Examination of the Raman spectral data is consistent with these

findings since there is little or no bR_{570} contribution to our M_{412} spectra and vice versa.

bR_{560} Measurements. For measurements on the dark adapted bR_{560} species, the sample (about 1.0 L of OD ~ 1.5) was dark adapted at room temperature for 24 h in advance. The sample was flowed through a stainless steel syringe needle of 0.30-mm diameter past a 3-mW 530.9-nm laser beam focused to 27 ± 2 μm diameter. The beam transit time was 3 μs in these experiments. The suspension was only passed through the laser beam once to ensure that the sample remained dark adapted throughout the measurement. In order to verify that the bacteriorhodopsin was not light adapted in these experiments, the laser beam was expanded to cover the whole width of the jet stream and a photon flux equivalent to a 3-mW 530.9-nm laser beam focused to 27 μm was delivered to the flowing sample. Absorption measurements on this sample verified that the bacteriorhodopsin remained essentially dark adapted after passage through the laser beam once at this low power level. These absorption measurements were performed within 3 min of the suspension being in the laser beam. This was done quickly to ensure that any light-adapted molecules would not have sufficient time to dark adapt since the $t_{1/2}$ of dark adaptation is 21 min. The resolution of the dark adapted bR_{560} Raman experiments was 3 cm^{-1}.

Flow System. The sample flow apparatus consisted of a recycling flow system driven by a small variable speed pump (Micro-pump Model 14-21-303). Bacteriorhodopsin (OD ≈ 1.0 on a 1-cm pathlength) was flowed through stainless steel flat syringe needles of varying diameter or through glass capillary tubes. A reservoir of about 20 mL was used throughout with the exception of the bR_{560} experiments. The reservoir was not cooled, but dry air was blown on the pump to minimize sample heating. The reservoir was illuminated with a 200-W flood lamp to ensure that the bacteriorhodopsin was light adapted for all measurements except for the bR_{560} case. The temperature of the sample was measured to be 29 °C near the point of laser excitation as monitored with a thermocouple attached to the syringe needles.

Sample Preparation. Fully deuterated and ^{15}N-enriched bacteriorhodopsin were a generous gift of H. Crespi of Argonne National Laboratories. These samples, as verified by the resonance Raman results, were greater than 95% enriched.

Halobacterium halobium (S9) was grown by the method of Kanner & Racker (1975). Their method for isolation of bacteriorhodopsin was followed except that we treated the bacteriorhodopsin vesicles to 1% deoxycholic acid (neutralized with NaOH to pH 8.0) three times followed by four doubly distilled water washings. One possible impurity that had to be eliminated from the bacteriorhodopsin samples was bacterial carotenoids from the red membrane of *Halobacterium halobium*. These carotenoids exhibit resonance Raman bands at 1001, 1157, and 1515 cm^{-1} as observed in spectra of whole cells. An acetone methanol extract of this carotenoid exhibits visible absorption bands at 468, 498, and 532 nm. We have found that these carotenoid bands are most resonance enhanced with 476.2-nm excitation. Sample purification procedures were reiterated (i.e., retreatment with deoxycholic acid which is effective in removing carotenoids) until there was no evidence of peaks at 1001, 1157, and 1515 cm^{-1} in either 77 K or room temperature resonance Raman spectra taken with 10 mW of 476.2-nm laser excitation. In addition, we have found that this procedure of washing with deoxycholic acid has no effect on either the spectral features of bR_{570} or the kinetics of formation of M_{412}. Sample purity was further checked by polyacrylamide gel electrophoresis which exhibited only a single protein band with an apparent molecular weight of

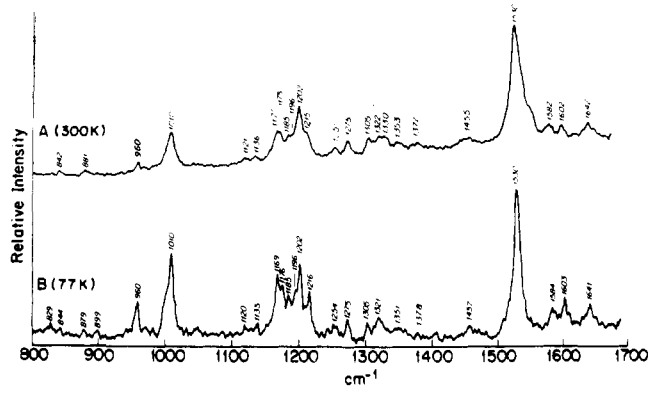

FIGURE 3: Resonance Raman spectra of (A) bR_{570} in doubly distilled H_2O (pH 6.6), OD 1.0 obtained with 30-mW of 530.9-nm laser light focused to 27 μm with a laser beam transit time of 500 ns. (B) A 77 K spectrum of bacteriorhodopsin obtained with 10 mW of 530.9-nm laser excitation. Resolution is 1 cm^{-1} in each case.

25 000 ± 2000. The absorption ratio A_{280}/A_{570} was found to be between 1.8 and 2.0 for purified sonicated bacteriorhodopsin preparations. The average yield of purified bacteriorhodopsin utilizing this procedure is about 25 mg per L of cell culture.

Bacteriorhodopsin analogues with fully deuterated membranes and protonated retinals or protonated membranes with fully deuterated retinals or 3-dehydroretinal as the chromophore were prepared as described previously (Marcus et al., 1977).

Crystalline *all-trans-N*-retinylidene-*n*-butylamine (NRB) was prepared as previously reported (Sulkes et al., 1976). The unprotonated Schiff bases of *all-trans*-3-dehydroretinal with butylamine and unprotonated Schiff bases of hexylamine, propylamine, and deuterated butylamine (d_9) with *all-trans*-retinal were prepared in a similar manner. The solutions of all-trans protonated Schiff bases were prepared by bubbling HBr gas through an ethanolic solution of the corresponding unprotonated Schiff base until the absorption spectrum showed complete protonation. The protonated and unprotonated Schiff bases of 13-*cis*-retinal were also prepared as above. The methylated Schiff base with butylamine ($N^+RB{\cdot}CH_3$) was formed by bubbling CH_3Br gas instead of HBr and the deuterated Schiff base of butylamine (N^+RBD) was prepared by bubbling DBr gas through a deuterioethanol (CH_3CH_2OD) solution of NRB. The final solutions of the protonated, methylated, and deuterated Schiff bases were at a concentration of 20 mM and were flowed at ~5 mL/s through 2-mm diameter capillary tubes. Spectra of the unprotonated Schiff base were obtained in acetonitrile. All the retinal isomers were purified using high pressure liquid chromatography before the preparation of Schiff bases. All procedures were carried out in dim red light.

Results

The kinetic and steady-state resonance Raman data obtained on bacteriorhodopsin are summarized in Figures 1 and 3-8. Figure 3A shows the resonance Raman flow spectra of bR_{570} in doubly distilled H_2O, pH 6.6, at a resolution of 1 cm^{-1} obtained with 30 mW of 530.9-nm excitation and a laser beam transit time of 500 ns. A 77K spectrum also obtained with 1 cm^{-1} resolution, where only bR_{570} and K_{610} are present, is shown in Figure 3B. Figure 4 shows a comparison of bR_{570} flow spectra obtained in H_2O and in D_2O. Both these spectra were run at lower resolution (3-4 cm^{-1}) than the bR_{570} spectra shown in Figure 3. A comparison between bR_{560}, bR_{570}, and the protonated Schiff base of *all-trans*- and 13-*cis*-retinal is

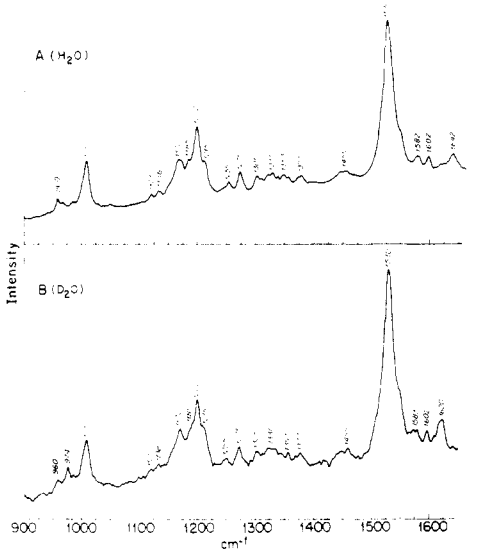

FIGURE 4: Resonance Raman spectra of bR_{570} in (A) H_2O and (B) D_2O. These spectra were obtained with 30 mW of 530.9-nm excitation and laser beam transit times of 1 μs.

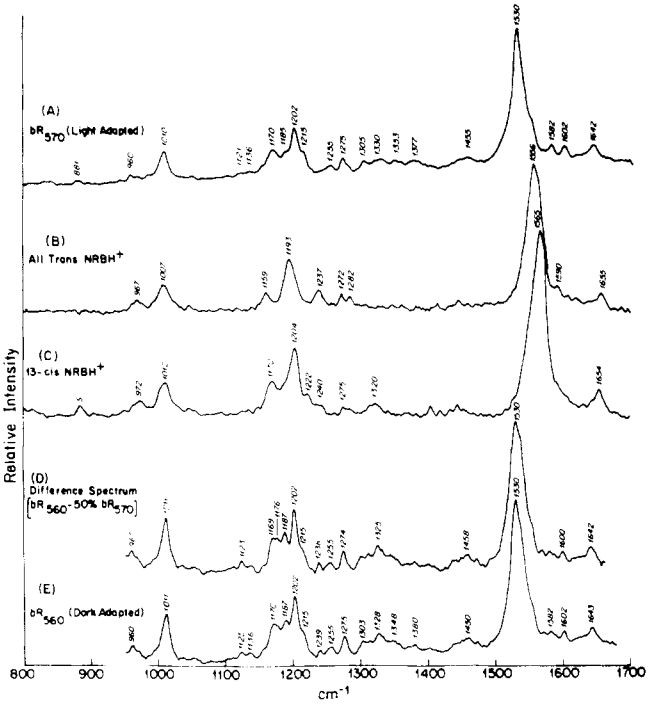

FIGURE 5: Resonance Raman spectra of (A) bR_{570}, (B) *all-trans*-N^+RBH, (C) 13-*cis*-N^+RBH, (D) difference spectrum [bR_{560} − 50% bR_{570}] and (E) bR_{560}. Resolution is 2 cm^{-1} in each case. Instrumental parameters are as described in the text.

shown in Figure 5. Figure 6 shows the resonance Raman spectrum of M_{412} obtained with the pump–probe flow technique. This spectrum was obtained with a pump beam of 300 mW of 573.0 nm laser light focused to 100-μm diameter 1.0 ms upstream in time from the 5-mW 457.9-nm probe beam. The pump and probe beams were focused to give beam transit times of 45 and 10 μs, respectively. The resolution in this case was 2.5 cm^{-1}. As a comparison the unprotonated Schiff bases of *all-trans*- and 13-*cis*-retinal are also shown in Figure 6.

Table I summarizes our Raman observations on bR_{570} and M_{412}. Included in this table are measured depolarization ratios for most of the observed bands. It is found that the depolarization ratio of all bands in bR_{570} and M_{412} is about 0.35. This is consistent with findings that for totally symmetric vibrations

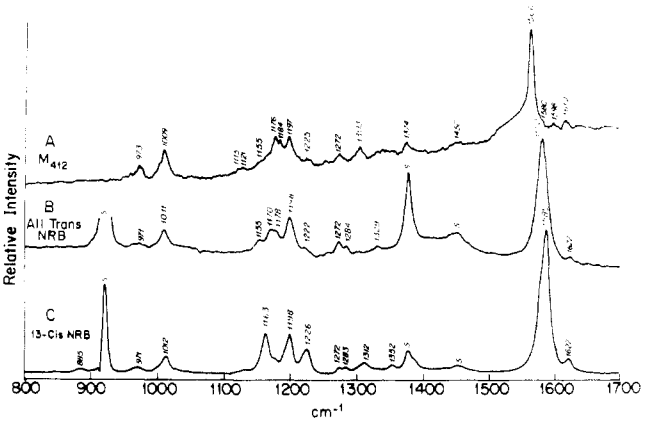

FIGURE 6: Resonance Raman spectra of (A) M_{412}, (B) *all-trans*-NRB and (C) 13-*cis*-NRB. Resolution is 2 cm^{-1} in each case.

$\rho = 1/3$ (Behringer, 1976).

Figure 7 shows resonance Raman spectra taken with 30 mW of 457.9-nm light for various transit times in the beam at pH 6.6 in doubly distilled water. In Figure 7A we show for comparison the resonance Raman spectrum of bacteriorhodopsin taken under steady-state conditions with the same excitation parameters. It is important to note that the steady-state mixture is highly dependent on pH and salt concentrations. Steady-state resonance Raman experiments on purple membrane as a function of pH and salt concentration have been performed. These results are summarized in Table II which lists the ratios of the C=C stretch of bR_{570} and M_{412} at 1530 and 1566 cm^{-1}, respectively. As can be seen an increase in pH from 5 to 10 results in increasing drastically the percentage of M_{412} in stationary state resonance Raman measurements obtained with 30-mW 488.0-nm excitation. Figure 7B shows the resonance Raman spectrum obtained with a beam transit time of 1 μs in an experiment utilizing the Pockels cell as described in the Materials and Methods. The data in Figure 7G were obtained simultaneously with the spectrum in Figure 7B and show a resonance Raman spectrum of almost pure M_{412} obtained with the pump beam on (500 mW of 580 nm, 500 μs upstream). This demonstrates the utility of the Pockels cell in performing experiments of this kind. Figures 7C–F show spectra obtained with beam transit times of 8, 18, 29, and 40 μs, respectively.

In Figure 1 are plotted theoretical curves of $\overline{C(t_f)}$ for various transit times in a 30-mW, 457.9-nm laser beam with the input optics used in these experiments (Figure 7). We also include experimentally observed concentrations for M_{412} as squares in the diagram. These concentrations were calculated in the following manner. We normalized the % M_{412} by assuming that the double beam M_{412} flow spectrum shown in Figure 6 contained 90% M_{412}. All spectra were taken with the same sample concentration and count time per channel. By comparing the relative number of counts in the 1566-cm^{-1} band, we were able to arrive at the percent composition of M_{412} in these spectra. The triangles show the intensities of the 1530 cm^{-1} band relative to the 1566 cm^{-1} bands normalized to M_{412} concentrations. Notice that the experimental M_{412} data points fit well on the theoretical curve. However, the bR_{570} data points all fall below the theoretical curve. This can be explained simply by the fact that the resonance Raman cross-sections for these two species are not the same at 457.9 nm. When we renormalize to the 1530-cm^{-1} band in the bR_{570} spectrum taken with a transit time of 500 ns, we then obtain the open circles in Figure 1 which fall on the bR_{570} curve. These data can be used to estimate the relative resonance enhancement

TABLE I: Observed Resonance Raman Peaks in bR_{570} and M_{412} and Depolarization Ratios of These Bands.[a]

bR_{570}	M_{412}	ρ	assignment
842		0.37 ± 0.20	
881		0.39 ± 0.20	
960		0.4 ± 0.10	C-C-H bend out-of-plane
	972	0.38 ± 0.15	C-C-H bend out-of-plane
	1009	0.40 ± 0.08	C_9-CH_3, C_{13}-CH_3 stretch
1010		0.40 ± 0.08	C_9-CH_3, C_{13}-CH_3 stretch
	1115		
1121	1121		[C_{14}-C_{15} stretch]
1136			
1170		0.34 ± 0.15	[C-C (C_9 to C_{13} stretch)]
1175		0.34 ± 0.15	
	1176	0.36 ± 0.20	
	1184	0.33 ± 0.21	
1185		0.40 ± 0.15	
1196		0.41 ± 0.15	[C-C stretch, CH_3 rock]
	1197	0.43 ± 0.15	
1202		0.34 ± 0.10	
1215		0.48 ± 0.20	
	1225	0.35 ± 0.20	isoprenoid chain motions in-
1255		0.29 ± 0.18	volving the Schiff base linkage
	1272		C—C—H bend + C=C
1275		0.34 ± 0.17	or C—C stretch
	1303		
1305			
1322			C_{13} methyl symmetric
1330			deformation region
1353			
	1374		C_9 methyl symmetric
1377		0.41 ± 0.20	deformation
	1450		asymmetric methyl defor-
1455			mation C_9 and C_{13}
1530		0.35 ± 0.06	C=C stretch
	1566	0.40 ± 0.10	C=C stretch
	1580		
1582		0.36 ± 0.18	
	1598		
1602		0.34 ± 0.20	
	1619	0.38 ± 0.18	C=N unprotonated stretch
1642		0.35 ± 0.15	$C=N^+H$ stretch

[a] Also included are peak assignments based mainly on the work of Cookingham et al. (1978). Tentative assignments are bracketed.

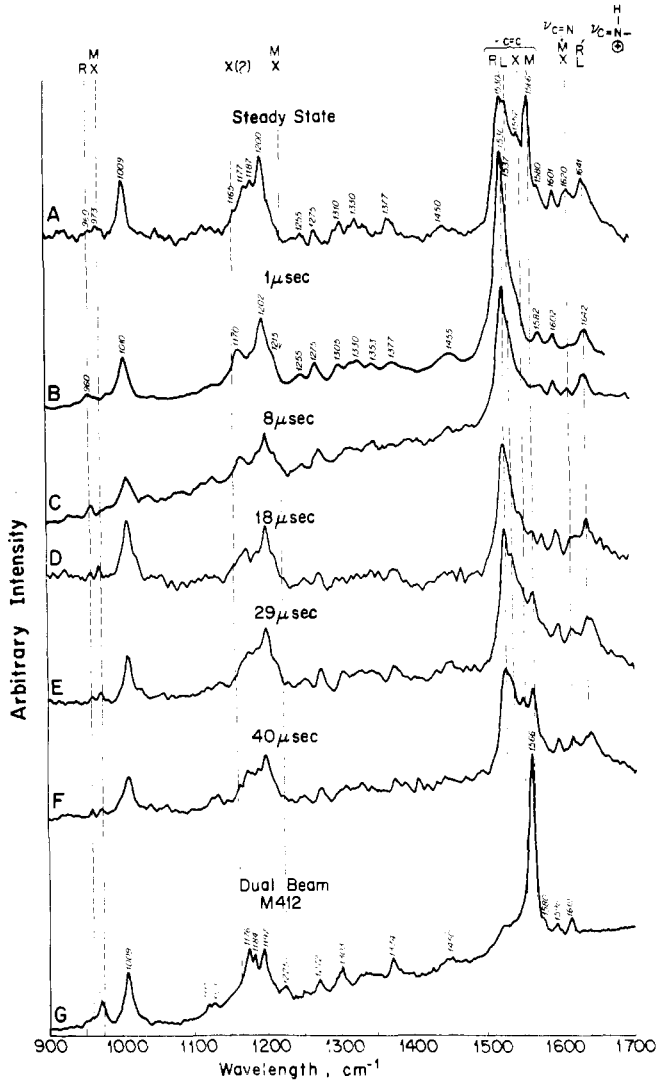

FIGURE 7: Resonance Raman spectra of bacteriorhodopsin obtained with 30 mW of 457.9 nm laser light focused to 23 μm for various transit times in the laser beam. (A) Steady-state and transit times of (B) 1 μs, (C) 8 μs, (D) 18 μs, (E) 29 μs, (F) 40 μs. (G) Dual laser beam spectrum of M_{412} obtained simultaneously with spectrum B utilizing the Pockels cell as described in the text.

ratio σ_R/σ_M at 457.9 nm. When this is done, it is found that the relative resonance enhancement ratio σ_R/σ_M at 457.9 nm is 0.77 ± 0.10. Discrepancies exist in the literature as to the true absorption spectrum of M_{412}. When these discrepancies are resolved, we will then be able to determine how the resonance enhancement ratio scales with extinction.

As a comparison to this 457.9-nm kinetic data, Figure 8 shows kinetic resonance Raman spectra obtained with 568.2-nm excitation and beam transit times of 5, 10, 25, 50, and 100 μs. Figures 9–11 contain resonance Raman spectra of molecular species which are necessary for our interpretations. In Figure 9 the resonance Raman flow spectra of various all-trans protonated and deuterated Schiff bases of retinal and an all-trans methylated Schiff base are shown. Figure 10 contains a low resolution M_{412} spectrum and a high resolution spectrum of the M_{405} species obtained in guanidine hydrochloride. Figure 11 compares the fingerprint regions of the M species of 3-dehydrobacteriorhodopsin with an unprotonated Schiff base of *all-trans*-3-dehydroretinal.

Discussion

Light-Adapted Bacteriorhodopsin (bR_{570}). The spectrum shown in Figure 3A was taken with 1-cm^{-1} resolution and 30 mW of 530.9-nm laser excitation with a sample residence time in the laser beam of ~500 ns. With this residence time and excitation geometry, it can be demonstrated (using calculations such as those used to obtain the theoretical curves shown in Figure 1) that the contribution to a resonance Raman spectrum should be about 95% bR_{570}. We note that the C=C stretch of bR_{570} occurs at 1530 cm^{-1} in agreement with earlier results (Lewis et al., 1974). This spectrum (see Figure 3A) also verifies that the -C=N- stretch in bR_{570} is at 1642 cm^{-1}. In addition,

TABLE II: Ratios of Heights of 1530 to 1566 cm^{-1} Bands as a Function of pH for Buffered and 4 M NaCl Solutions of Bacteriorhodopsin.[a]

	pH 5	pH 7.5	pH 10.0
0.1 M buffer	1.79	0.72	1.00
4 M NaCl + buffer	1.92	0.49	0.47

[a] The spectra were taken with 30 mW of 488.0-nm laser excitation. The pH 5 and pH 7.5 samples were buffered with 0.1 M PO_4^{2-} and the pH 10 samples were buffered with CO_3^{2-}.

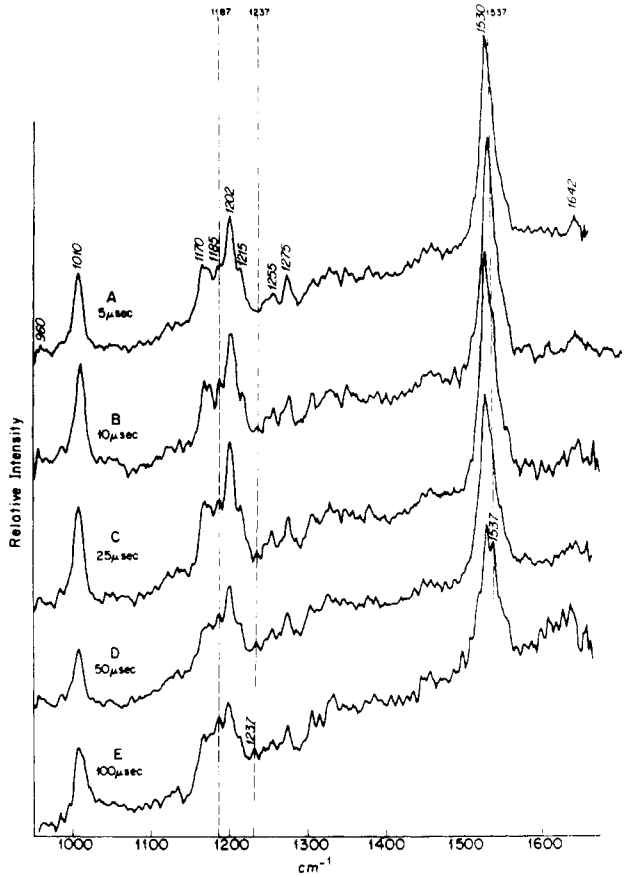

FIGURE 8: Kinetic resonance Raman spectra of bacteriorhodopsin obtained with 50 mW of 568.2-nm excitation and laser beam transit times of (A) 5 μs, (B) 10 μs, (C) 25 μs, (D) 50 μs, and (E) 100 μs.

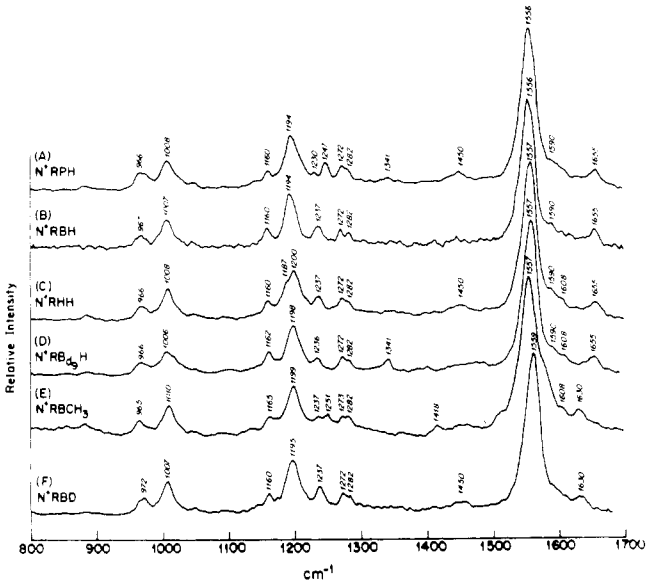

FIGURE 9: Resonance Raman spectra of *all-trans*- (A) N^+RPH, (B) N^+RBH, (C) N^+RHH, (D) $N^+RB_{d9}H$, (E) N^+RBCH_3 and (F) N^+RBD. These spectra were obtained with 15 mW of 476.2-nm excitation with 2-cm^{-1} resolution. Ethanol was the solvent in each case and the sample was flowed as discussed in the text.

it can be shown that the effect of resuspending bacteriorhodopsin in D_2O reduces the frequency of the C=N stretch from 1642 to 1620 cm^{-1} (see Figures 4A and 4B). This is consistent with earlier steady-state results (Lewis et al., 1974) and indicates that there is a proton on the Schiff base.

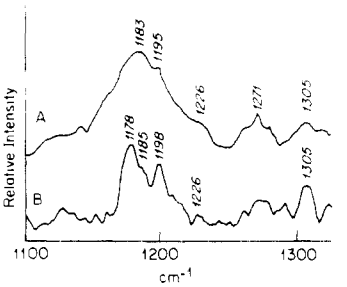

FIGURE 10: Resonance Raman spectrum of (A) M_{412} taken with 11-cm^{-1} resolution and (B) the M_{405} intermediate in guanidine hydrochloride treated bacteriorhodopsin obtained with 2-cm^{-1} resolution.

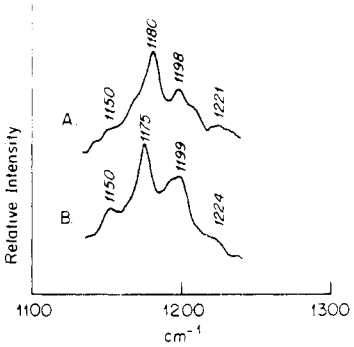

FIGURE 11: Resonance Raman spectra of (A) M intermediate of 3-dehydrobacteriorhodopsin and (B) *all-trans*-3-dehydro-NRB. The unlabeled shoulders in spectrum (A) correspond to vibrational features from other intermediates as determined by the excitation frequency dependence. These additional features arise since spectrum A was obtained under steady-state conditions.

A. *The C-C-H Bending Region (950-990 cm^{-1}).* An interesting result of this investigation is the fact that none of the other major bands in the bR_{570} spectrum are affected by resuspension in D_2O except for the 960-cm^{-1} band which has been assigned to C-C-H out-of-plane bends. This vibration becomes weaker and another band appears at 975 cm^{-1} upon deuteration of the external medium. Such a frequency alteration upon deuteration of the medium suggests that this mode must be coupled in some manner to the Schiff base linkage (the only exchangeable group on the chromophore). Support for this hypothesis comes from comparing the C-C-H bends in protonated (N^+RBH) and deuterated (N^+RBD) Schiff bases of butylamine complexed to *all-trans*-retinal. As is seen in the resonance Raman spectra of these species the band profile of the C-C-H bends at 967 cm^{-1} in N^+RBH (Figure 9b) shifts up in frequency by ~5 cm^{-1} upon deuteration of the retinal Schiff base model (see Figure 9f). Although the frequency upshift in the models is not as great as suspending bacteriorhodopsin in D_2O, it is in the same direction. This difference in magnitude may be related to protein interactions at the Schiff base which will be discussed below.

Our hypothesis coupling the Schiff base linkage to the C-C-H bends on the polyene is further supported by comparing the 950-990-cm^{-1} region in ^{15}N-enriched bacteriorhodopsin with native bacteriorhodopsin both suspended in either H_2O or D_2O (see Table III). In ^{15}N-enriched bacteriorhodopsin the 960-cm^{-1} band is split into two components of about equal intensity at 960 and 969 cm^{-1}. Upon deuteration of the Schiff base the 969-cm^{-1} feature moves up in frequency to 985 cm^{-1}, whereas the 960-cm^{-1} component is unaffected. However, M_{412}, which has an unprotonated Schiff base (Lewis et al., 1974), exhibits a single C-C-H bend at about 973 cm^{-1}

even upon D_2O suspension and/or ^{15}N enrichment. Thus, these results lead to the conclusion that the 960-cm^{-1} band in bR_{570} is composed of *at least* two components. One component is a C-C-H bend which is unaffected by deuteration of the external medium or changing the mass of the Schiff base nitrogen, while the second component can be altered by deuterating the Schiff base and/or changing this Schiff base nitrogen's mass.

We note that the above frequency upshift, which is detected in certain components of the 960-cm^{-1} band upon resuspension in D_2O and/or ^{15}N enrichment, is in the wrong direction for a simple mass effect. One possible hypothesis which could account for these data is that the chromophore contains a series of C-C-H bends which are accidentally degenerate at 960 cm^{-1} in native bacteriorhodopsin. This degeneracy could be composed of several components including the $H-C_{15}$ bend in the $H-C_{15}=N^+H$ group. Deuteration or changing the Schiff base nitrogen's mass would shift the frequency of this bend giving rise to a new $H-C_{15}$ component at a higher frequency. Such frequency upshifts upon deuteration of neighboring groups have been observed previously in other highly coupled systems (Craig & Overend, 1969). The remaining band at 960 cm^{-1} from the other C-C-H bends on the isoprenoid chain would be essentially unaltered in frequency and weaker in intensity (as is observed in Figure 4B) if these vibrational modes were significantly less intense than the C-C-H bends near the Schiff base nitrogen.

B. *The Fingerprint Region (1100–1400 cm^{-1}).* To further resolve the spectral features of bR_{570}, spectra were obtained at 77 K (see Figure 3B). At this temperature and excitation conditions (Figure 3B), the steady-state concentration would be about 70% bR_{570} and 30% K_{610}. In addition resonance enhancement favors bR_{570} and, except for a temperature induced narrowing of all bands as compared with the room temperature flow data, we have not been able to resolve any vibrational modes that can be ascribed exclusively to K_{610}. This is supported by dual beam experiments in which a pump beam was used to enhance the concentration of K_{610} while a weaker probe beam excited the resonance Raman spectra, although these dual beam experiments (514.5 nm probe/615.0 nm pump or 514.5 nm pump/590.0 nm probe) did indicate that the intensities of the 1530- and 1202-cm^{-1} bands decrease while the 967-cm^{-1} band increases when K_{610} is present. The decrease in the 1530-cm^{-1} band could indicate that K_{610} has a C=C stretch at a different vibrational frequency and this is supported by recent kinetic resonance Raman data on fully deuterated bacteriorhodopsin in H_2O (Ehrenberg & Lewis, unpublished observations). It is also interesting to note in this regard that an intensity decrease in the ratio of the 1202-cm^{-1} band relative to the 1185-cm^{-1} band is detected when L_{550} is produced (as will be discussed later in this paper). This may indicate that structural adjustments first detected in the production of K_{610} persist and grow in magnitude in L_{550}. Thus, our data do indicate that small structural adjustments are occurring in the retinylidene chromophore in going from bR_{570} to K_{610}. However, there is no evidence to suggest that these structural adjustments include a photochemically driven trans to cis or cis to trans isomerization.

As discussed above the comparison of the room temperature and 77 K spectra indicates a general narrowing of all bands as the temperature is lowered, and this enables us to resolve bands in the structurally sensitive fingerprint region (1100–1250 cm^{-1}) which appear only as shoulders at room temperature (compare Figures 3A and 3B). We observe fingerprint bands at 1169, 1175, 1185, 1196, 1202, and 1215 cm^{-1} when spectra are taken with 1-cm^{-1} resolution (Figure 3A) at room temperature. We also note that at liquid nitrogen temperature four bands occur in the 800–900-cm^{-1} region at 829, 844, 879, and 899 cm^{-1}, while at room temperature only the bands at 842 and 881 cm^{-1} are resolved in this frequency region.

TABLE III: Observed Bands in the 950–990-cm^{-1} Region in Bacteriorhodopsin and ^{15}N-Enriched Bacteriorhodopsin Suspended in H_2O and D_2O.[a]

		H_2O	D_2O
native bR	bR_{570}	960	975, 959
	M_{412}	972	973
^{15}N-enriched bR	bR_{570}	969, 960	985, 960
	M_{412}	973	973

[a] When more than one band is observed for a given species, the most intense band is listed first. The complete ^{15}N-enriched bacteriorhodopsin spectra will be reported elsewhere.

The fingerprint region has been found to be extremely sensitive to the conformation of retinal (Cookingham et al., 1976; Gill et al., 1970; Heyde et al., 1971; Lewis et al., 1973, 1974; Rimai et al., 1970). Sulkes et al. (1976) demonstrated that the resonance Raman spectrum of squid acid metarhodopsin is modeled well by a crystalline all-trans protonated Schiff base, and Mathies et al. (1977) have shown that the resonance Raman spectrum of rhodopsin is modeled better, although not exactly by 11-cis rather than 9-cis protonated Schiff bases of retinal with the reverse being true for isorhodopsin. All these findings are in agreement with the available biochemical evidence obtained by extracting the chromophores and analyzing their isomeric state by chromatography. In the case of bacteriorhodopsin biochemical extraction procedures yield exclusively *all-trans*-retinal as the configuration of the chromophore in bR_{570}. The only other retinal isomer implicated in bacteriorhodopsin's photochemistry is 13-cis. In dark-adapted bR_{560} a 1:1 mixture of 13-*cis*- and *all-trans*-retinal is found upon extraction (Oesterhelt et al., 1973; Pettei et al., 1977). Even though biochemical extractions of bR_{570} yield exclusively *all-trans*-retinal, the modeling of bR_{570} with protonated Schiff bases does not seem to be unique. In fact an exact correspondence of bR_{570} fingerprint bands with either of the two retinal protonated Schiff base isomers implicated in bacteriohodopsin's photochemistry cannot be made (see Figures 5A–C).

C. *Why Do Attempts at Modeling bR_{570} Fail?* One suggestion which can be discounted is the contribution of protein residues to scattering in the fingerprint region. This suggestion can be rejected on the basis of recently reported experiments incorporating protonated retinal into fully deuterated bacterioopsin (Marcus et al., 1977). These results show that the fingerprint region was unaffected by changing the isotopic nature of bacterioopsin (chromophore free bacteriorhodopsin). If protein bands contributed to the scattering, the spectrum should have been altered by fully deuterating the bacteriorhodopsin protein. In view of these data, the most likely explanation for the occurrence of extra peaks in the bR_{570} spectrum as compared with published spectra of all-trans protonated Schiff bases of retinal is the effect of the membrane environment on the chromophore. This is certainly consistent with the biochemical evidence since these experiments, unlike resonance Raman spectroscopy, are only sensitive to the double bond configuration of the free chromophore. If indeed this explanation is correct, then the observation of additional normal modes in bR_{570} must arise from a perturbation in a region of the chromophore which is far from the β-ionone ring.

TABLE IV: Isotopic Effects on Schiff Base Bands in Bacteriorhodopsin in H_2O (C=N and C=N+H) and D_2O (C=N and C=N+D) at pH 6.6.[a]

	-C=N- (cm^{-1})	C=N+H (cm^{-1})	C=N+D (cm^{-1})
H-retinal models	1622	1655	1630
H-retinal + H-opsin	1619	1642	1620
H-retinal + D-opsin	1618	1635	
D-retinal + H-opsin	1595	1625	
D-retinal + D-opsin	1594	1620	1592
H-retinal + H-opsin (^{15}N)	1614	1627	1613

[a] H = protonated; D = deuterated; ^{15}N = ^{15}N enriched.

This is indicated by the invariance of certain fingerprint region bands in the resonance Raman spectrum of 3-dehydrobacteriorhodopsin (Marcus et al., 1977).

Let us now consider what environmental factors could give rise to bands in the bR_{570} spectrum which are not present in the spectra of free protonated Schiff bases of *all-trans*-retinal. Previous workers (Aton et al., 1977) have implicity assumed that bacteriorhodopsin bR_{570} should be modeled by a simple protonated Schiff base of retinal. However, in model compounds the protonated Schiff base band occurs at 1655 cm^{-1}. This is also the case in rhodopsin, isorhodopsin, and squid acid metarhodopsin and it is interesting that these pigments are modeled fairly well by their respective simple protonated Schiff bases (Sulkes et al., 1976; Mathies et al., 1977). On the other hand, the analogous band in bacteriorhodopsin occurs at 1642 cm^{-1}, 13 cm^{-1} lower in frequency than in the models. This could indicate that the simple protonated Schiff base model for *bacteriorhodopsin* is not correct.

Support for the above hypothesis is seen in Table IV which shows the position of the carbon–nitrogen stretch in a series of protonated (H), deuterated (D), and ^{15}N-enriched bacteriorhodopsin samples. Notice that the frequency of the *unprotonated* Schiff base band is essentially the same in model compounds (1622 cm^{-1}) and in the purple membrane (1619 cm^{-1}) and is unaffected by deuterating the protein (bacterioopsin). This can be seen by comparing the frequency of the unprotonated C=N stretch when H- or D-retinal are complexed respectively to H- and D-bacterioopsin. On the other hand, the frequency of the *protonated* Schiff base carbon–nitrogen stretch is affected by the isotopic nature of the protein (e.g., compare in Table IV H-opsin or D-opsin complexed with H-retinal, 1642 cm^{-1} and 1635 cm^{-1}, respectively).

There is no indication that the effect on the protonated Schiff base band in deuterated bacterioopsin arises from the mass effect of the deuterated lysine side chain. This is indicated by the fact that the C=N+H vibrations in model compounds are unaffected when protonated retinal is complexed to fully deuterated butylamine or when the length of the hydrocarbon chain to which the Schiff base linkage is attached is altered. This is seen in Figures 9A–D (for the C=N+H vibration) which show spectra of protonated Schiff bases of hexylamine, butylamine, propylamine, and fully deuterated butylamine. In each case the C=N+H stretch occurs at 1655 cm^{-1}.

Thus, some other explanation is necessary to explain the effect of the protonated Schiff base band moving down in frequency upon deuterating the protein. A plausible suggestion is that a noncovalently linked protein group or groups in the vicinity of the Schiff base linkage interact with the protonated Schiff base but not the unprotonated Schiff base. Such an interaction through the Schiff base proton could explain both the observed effect on the C=N+H vibration and the lack of an effect on the -C=N- vibration. It could also account for the perturbation of the all-trans fingerprint vibrational structure in bR_{570} by causing changes in the nature of the Schiff base substituent (including changes in the state of protonation of Schiff base, mass changes, etc.). In a preliminary attempt to test this hypothesis, spectra of an all-trans methylated Schiff base were obtained (Figure 9E) and as can be seen certain spectral features in this compound such as the 1165- and 1251-cm^{-1} bands are indeed closer in frequency to features in the bR_{570} spectrum than any of the simple protonated models.

Thus, in summary the resonance Raman data on bR_{570} will agree with the biochemical evidence on the isomeric state of the chromophore when a model compound is synthesized which correctly accounts for all of the membrane-chromophore interactions. This not only includes interactions at the Schiff base but also includes alterations in Franck–Condon factors in and out of the membrane. As has already been noted in the modeling of rhodopsin and isorhodopsin (Mathies et al., 1977), these Franck–Condon factors have a significant effect on the observed resonance Raman intensities in and out of the protein environment. Therefore, it is clear that, although no protein bands are occurring in the spectrum, the protein environment does strongly influence the character of the vibrational spectrum of the all-trans chromophore in bR_{570}.

Dark-Adapted Bacteriorhodopsin (bR_{560}). Figure 5E shows the spectrum of dark-adapted bacteriorhodopsin (bR_{560}) obtained with the single pass flow method described in Materials and Methods. The spectrum is very similar to that of light-adapted bR_{570} except for a few changes occurring in the fingerprint region. A new band is observed at 1238 cm^{-1}, and there is much more intensity as well as a clearly resolved peak at 1187 cm^{-1}. The C=C stretch still occurs at about 1530 cm^{-1}, and bR_{560} has a protonated Schiff base linkage as observed by the invariance of the 1642-cm^{-1} band. Biochemical extractions have determined that the chromophore of bR_{560} is a 1:1 mol mixture of all-trans and 13-cis chromophores (Oesterhelt et al., 1973; Pettei et al., 1977). Thus, in order to observe the spectrum of the 13-cis component without complications from the bR_{570} species, we have subtracted a 50% contribution from the bR_{570} spectrum. This 13-cis chromophore difference spectrum is shown in Figure 5D. Here we observe more intensity at 1187 and 1238 cm^{-1} as expected, based on a comparison of bR_{560} and bR_{570} spectra (see Figures 5A and 5D). We also observe a larger band at 1325 cm^{-1}. This last feature has been assigned to the C_{13} methyl symmetric deformation (Cookingham et al., 1978) and is similar to a spectral component in a 13-cis protonated Schiff base of retinal (see Figure 5C). However, the modeling with the fingerprint region for the 13-cis pigment spectrum is not unique as is the case with bR_{570} for the all-trans model. This probably also arises from the protein–Schiff base secondary interactions discussed above when we analyzed the bR_{570} spectrum.

By comparing the resonance Raman spectra of bR_{560}, bR_{570}, and model compounds, it can be argued that the structural transformations involved in this transition are occurring near the end of the isoprenoid chain. Cookingham et al. (1978) have already noted that the region between 1220 and 1260 cm^{-1} has an extra band in Schiff bases which is not present in the retinals. The vibrational frequency of this mode shifts from 1237 to 1222 cm^{-1} when protonated and unprotonated Schiff bases of butylamine are compared (compare Figures 5B with 6B and 5C with 6C). This together with the lack of such a band in the retinals indicated (Cookingham et al., 1978) that the normal coordinate includes motions of atoms at the end of the iso-

prenoid chain. Such an assignment is further supported by the data presented in Figure 9 in which the end group is varied from propyl to hexyl and the vibrational frequency of this mode is altered from 1247 to 1236 cm^{-1}. Thus changes in vibrational modes in this region can monitor alterations in the end of the isoprenoid chain.

In view of these observations and the previous discussion of an interaction at the Schiff base, it is significant that instead of a 1237-cm^{-1} band which normally is observed in protonated butylamine Schiff bases, a band of similar intensity in this region occurs in bR_{570} at 1255 cm^{-1}. Furthermore in bR_{560} a new band arises in this region at 1238 cm^{-1}, and it is interesting that $N^+RB(CH_3)$ also has two bands at 1237 cm^{-1} and 1251 cm^{-1} in this region (see Figure 9). All these facts indicate that the structural alterations in the thermal transition from bR_{570} to bR_{560} involve motion about the end of the isoprenoid chain.

M_{412}. The rate of development of M_{412} can be monitored by the observation of the C=C stretch at 1566 cm^{-1} (see Figure 7). This band has previously been associated with the M_{412} species (Lewis et al., 1974). It can be shown that the time development of this band matches the theoretical curve of Figure 1. These theoretical curves are based on data of other workers (Lozier et al., 1975; Kung et al., 1975) using transient absorption spectroscopy. Our Raman data are seen to be in agreement with their findings on the onset of the absorption of M_{412}.

The resonance Raman spectrum of M_{412} shown in Figure 6 was obtained at physiological pH by the dual beam technique. We used 5 mW of 457.9-nm light with a probe beam transit time of 10 μs. Under these excitation conditions effects of possible light driven reactions from M_{412} are minimized as in the case of obtaining a spectrum of pure bR_{570}. We estimate that M_{412} contributes greater than 90% to the observed resonance Raman spectrum as evidenced by the single C=C stretch at 1566 cm^{-1}. This is also indicated by the absorption measurements (discussed in Materials and Methods) using this dual laser beam geometry. The slight asymmetry on the low energy side of this band may be due to minor contributions from the intense C=C stretches of other intermediates.

It is observed that the M_{412} spectrum (see Figure 6) is quite different than the spectrum of bR_{570} (see Figure 5A). The bR_{570} band at 960 cm^{-1} shifts up in frequency to 972 cm^{-1} in M_{412}. The C=N stretch shifts down from 1642 cm^{-1} in bR_{570} to 1619 cm^{-1} in M_{412}. This is consistent with the observation that the Schiff base linkage in M_{412} is unprotonated (Lewis et al., 1974). In the fingerprint region of M_{412} we observe bands at 1155, 1176, 1184, 1197, and 1225 cm^{-1}. These bands are distinct from those observed in bR_{570}. In bR_{570} there is a weak doublet at 1121 and 1136 cm^{-1}, whereas in M_{412} a weak doublet occurs at 1115 and 1121 cm^{-1}. In addition differences in the spectral features of these species are also observed between 1300 and 1370 cm^{-1} as well as between 1400 and 1500 cm^{-1}. These regions include the symmetric C_{13} methyl deformation and asymmetric methyl deformations respectively (Cookingham et al., 1978), and probably are reflecting changes in the state of protonation. On the other hand some spectral features such as the 1010 C-CH_3 stretch, the 1374, 1580, and 1600 cm^{-1} bands are essentially unaltered in going from bR_{570} to M_{412}. Based on the work of Cookingham et al. (1978) the 1374-cm^{-1} band in M_{412} (1378 cm^{-1} in bR_{570}) can be assigned to a C_9 methyl symmetric deformation. The similar frequency of this band in bR_{570} and M_{412} could indicate that the interactions in the vicinity of the C_9 methyl group are similar in both species and/or the state of isomerization of the chromophore is the same.

Recently Aton et al. (1977) have also obtained the resonance Raman spectrum of M_{412} utilizing a method based on chemically slowing down the return of M_{412} to bR_{570}. This was done by suspending bacteriorhodopsin in 4 M salt at high pH (pH 10.0). At first sight their spectrum and our spectra, especially in the fingerprint region (between 1100 cm^{-1} and 1250 cm^{-1}) which has closely spaced vibrational structure, appear to be quite different. However, their spectrum was obtained with 11 cm^{-1} resolution, whereas all the data reported in this paper was obtained with 2 cm^{-1} resolution. Thus, their spectrum obscured certain important details of the M_{412} spectrum which are critical in trying to model the isomeric state of the chromophore. To illustrate our point Figure 10A shows the fingerprint region of a sample with a high concentration of M_{412} obtained with 11-cm^{-1} resolution. This spectrum is in agreement with the results reported by Aton et al. As is expected for a spectrum with bands of different widths and intensities the band profile is seriously altered when compared with our higher resolution data. Figure 10B shows the fingerprint region of a guanidine hydrochloride–bacteriorhodopsin (pH 10) sample obtained with 457.9-nm excitation and 2-cm^{-1} resolution. In guanidine hydrochloride, the M-like intermediate (λ_{max} = 405 nm) is known to have a 13-cis chromophore (Pettei et al., 1977). In view of the data in Figures 10A and 10B, it is understandable that Aton et al. concluded that M_{412} has a 13-cis chromophore.

In Figure 6 is found a comparison of the M_{412} spectrum with model unprotonated Schiff bases of *all-trans*- and 13-*cis*-retinal. Our data clearly disagree with the conclusions of Aton et al. who implied that the spectrum of M_{412} corresponds more closely to the 13-cis model compound (see Figures 6A and 6C). Our data, on the other hand, demonstrate that there are close agreements in the fingerprint region between M_{412} and the all-trans model compound (see Figures 6A and 6B). Notice, for example, the splitting at 1176 and 1184 cm^{-1} in M_{412} and the corresponding split components at 1170 and 1178 cm^{-1} in the all-trans unprotonated Schiff base. It is significant that these components are completely absent in the 13-cis model compound. Also notice the close correspondence between the intense 1197-cm^{-1} band and the weak 1225-cm^{-1} band with similar spectral features at 1198 cm^{-1} and 1222 cm^{-1} in the all-trans model. Furthermore, there is a weak band in *all-trans*-NRB at 1155 cm^{-1} with corresponding scattering observed in this region in our M_{412} spectrum. Even though this is in a region where carotenoid impurities in bacteriorhodopsin have large peaks, we feel confident that this is a true M_{412} feature, since no scattering is observed at 1155 cm^{-1} in our guanidine hydrochloride M_{405} spectrum obtained with the same bacteriorhodopsin sample (see Figure 10B). These results lead us to conclude that the isomeric state of the chromophore in M_{412} is essentially all-trans.

In order to further test this conclusion we have obtained the resonance Raman spectrum of the M_{412} analogue ($\lambda_{max} \sim 440$ nm) of 3-dehydrobacteriorhodopsin (see Figure 11A). Because of the extra double bond in the β-ionone ring of the chromophore, the absorption maximum of the M intermediate of this analogue is closer to that of available laser lines (457.9 nm). Therefore, the resonance enhancement factors are such that when a stationary sample of 3-dehydrobacteriorhodopsin is excited with 457.9-nm laser light the spectral features of the M intermediate predominate (Marcus et al., in preparation). Figure 11 compares the conformationally sensitive fingerprint region of the M intermediate of 3-dehydrobacteriorhodopsin with a spectrum of an unprotonated Schiff base of *all-trans*-3-dehydroretinal. Notice the close correspondence in frequency and intensity between these two spectra. Thus we feel confident

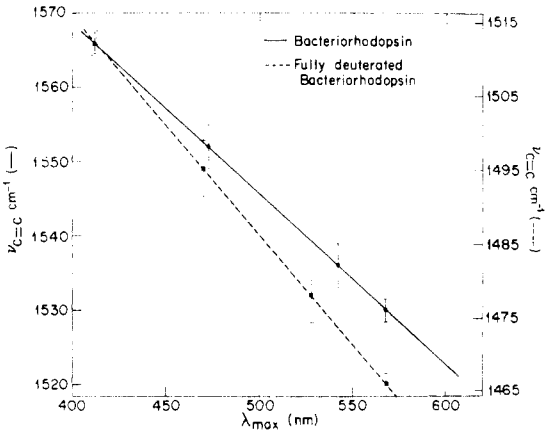

FIGURE 12: Linear correlation plots of $\nu_{C=C}$ vs. λ_{max} for bacteriorhodopsin (solid line) and fully deuterated bacteriorhodopsin (dashed line).

that the chromophore in the M intermediate is indeed in an all-trans isomeric state.

In view of this conclusion it is important to consider the controversy that has existed on the conformational state of the M intermediate based on biochemical extraction procedures. Unlike the relatively stable bR_{570} species the M_{412} intermediate normally decays rapidly (ms) at temperatures at which extraction procedures have been performed. Thus, in order to extract the M_{412} chromophore, organic compounds have been utilized to alter the kinetics and thus slow down the regeneration of bR_{570}. These organic compounds such as ether (Jan, 1975), dimethyl sulfoxide (Oersterhelt et al., 1973), methylene chloride (Pettei et al., 1977), and guanidine hydrochloride (Pettei et al., 1977) are reagents which are known to disrupt membrane and protein structure. Even though this is the case, these have been the only biochemical procedures thus far which could give information on the isomeric state of the chromophore *in an unstable protein conformation such as* M_{412}. Thus, it is not surprising that data obtained with the above reagents yield different results. In fact experiments reported from the same laboratory (Pettei et al., 1977) with different reagents give different results. Pettei et al. report that when methylene chloride and ether are used a 1:1 all-trans/13-cis ratio is obtained for the M_{412} chromophore whereas with the addition of guanidine hydrochloride at high pH exclusively 13-cis is extracted.

It should be pointed out that the absorption maximum of the intermediate which presumably corresponds to M_{412} in guanidine hydrochloride has an absorption maximum which does not coincide with the physiologically active M intermediate. In fact the absorption of the species in guanidine hydrochloride is 405 nm, 7 nm blue shifted from M_{412}. In this regard it should be noted that a change in isomeric state from all-trans to 13-cis in this protein is known to blue shift the absorption maximum. This is observed in the bR_{570} to bR_{560} transition. Furthermore, we have obtained the resonance Raman spectrum of the M species in guanidine hydrochloride treated bacteriorhodopsin at pH 10. The fingerprint region of this species is shown in Figure 10B. We note that this spectrum is distinct from the spectrum of M_{412} obtained at physiological pH (e.g., in Figures 6 and 10 notice that the 1155-cm^{-1} scattering in M_{412} is absent in M_{405}; intensity of the 1176-cm^{-1} band relative to the 1184-cm^{-1} band has changed in going from M_{412} to M_{405}).

In summary all these biochemical procedures are not sensitive to the in situ structure and interactions of the chromophore with its protein environment. Resonance Raman spectroscopy as we have shown is the only reported technique that is sensitive to both the structure and the interactions of the chromophore in situ. Thus, even though the biochemical evidence is in conflict we still must conclude based on our resonance Raman data that the structure of the isoprenoid chain in M_{412} is all-trans. However, it should be pointed out, based on our analysis of the bR_{570} spectrum, that the vibrational features of a chromophore in a highly coupled protein complex could be misleading. Therefore, a definitive structural assignment will have to await the synthesis of a model compound which accurately represents the active site of bacteriorhodopsin.

Other Intermediates in the Photochemical Cycle of Bacteriorhodopsin. Figure 7A shows a steady-state resonance Raman spectrum of bacteriorhodopsin obtained with 30 mW of 457.9-nm light. We note that C=C stretching vibrations occur in this spectrum which cannot be attributed to either bR_{570} or M_{412}. These bands occur at 1537 and 1552 cm^{-1}, respectively. By examining the kinetic flow spectra seen in Figures 7B–7F we note the following trends. At short times a shoulder appears at about 1537 cm^{-1} which is a discernible peak in the spectrum obtained with a beam transit time of 29 μs (see Figure 7E). This band also occurs with additional intensity in kinetic resonance Raman flow spectra obrained with 50 mW of 568.2-nm excitation as the sample residence time in the laser beam is increased (see Figure 8A–E). In addition increasing the laser sampling time with 457.9-nm excitation results in a second band at 1552 cm^{-1} which can only be observed as a weak shoulder when the transit time is increased with 568.2-nm excitation (compare Figures 7 and 8). Both these bands clearly grow in intensity earlier in time than the 1566-cm^{-1} C=C stretch of M_{412}, but their kinetics and resonance enhancements appear to be different. These results suggest that we are time resolving bands due to two different photochemical intermediates which occur before M_{412}.

Assignment of the 1537 cm^{-1} and 1552 cm^{-1} C=C Stretches. Electron delocalization appears to be related to the absorption maximum of bacteriorhodopsin and its photochemically induced intermediates. Coupled to an increase in electron delocalization is a decrease in double bond order resulting in a lowering of the C=C stretching frequency. Hence, there is a good correlation between λ_{max} and $\nu_{C=C}$ in relaxed retinylidene chromophores (Rimai et al., 1971). Thus, we use this type of a correlation as a guide in assigning C=C stretches to various intermediates in the bacteriorhodopsin photochemical cycle.

The only known intermediates between bR_{570} and M_{412} are K_{610} and L_{550}. K_{610} occurs within 1.0 ± 0.5 ps (Lewis et al., 1977; Ippen et al., 1978) and decays in about 2 μs at room temperature (Lozier et al., 1975). Due to its low average concentration in the laser beam at room temperature (Figure 1) and unfavorable resonance enhancement factors at 457.9 nm, we do not expect to observe any K_{610} in our kinetic resonance Raman spectra shown in Figure 7. Therefore, we do not believe that any of the observed C=C stretches arise from K_{610}. Thus, the only *known* intermediate to which we can assign the additional C=C stretches observed at 1537 and 1552 cm^{-1} is L_{550}. However, the kinetic resonance Raman results suggest that these two bands arise from different species. This is based on their different rates of appearance and different excitation frequency dependence (compare Figures 7 and 8).

In order to assign these two C=C stretches to distinct species we now make use of the observed correlation between $\nu_{C=C}$ and λ_{max} discussed above. Figure 12 plots all the C=C stretching frequencies observed in our data vs. absorption maxima in wavelength with the bR_{570} and M_{412} C=C

stretches used as the reference points in drawing the straight line. Based on this diagram (Figure 12, solid curve) a C=C stretch of 1537 cm^{-1} correlates well with a λ_{max} between 530 and 555 nm. Thus, it seems reasonable to assign the 1537-cm^{-1} band to the C=C stretch of L_{550}. On the other hand, the band at 1552 cm^{-1} which was previously assigned to L_{550} (Campion et al., 1977) correlates well with an absorption maximum between 460 and 485 nm. Thus, we suggest that a new intermediate which we call X (λ_{max} between 460 and 485 nm) appears before the M_{412} intermediate.

Support for these assignments can be found in steady-state resonance Raman measurements obtained as a function of frequency. The excitation frequency dependence of the steady-state measurements reveals that the 1552-cm^{-1} C=C stretch is most resonance enhanced at about 746.5 nm. This is consistent with the absorption of this species X obtained from the correlation diagram in Figure 12. In addition, further support for this correlation and our assignments can be found in an analysis of the resonance Raman spectrum of bacteriorhodopsin grown in fully deuterated media. Measurements at 95 K on this species show a single C=C stretch at 1466 cm^{-1} which can be assigned to bR_{570}. As the temperature is raised C=C stretches start occurring at 1478, 1495, and 1512 cm^{-1}. This latter feature is best resonance enhanced with blue lines and can be assigned to M_{412} using room temperature steady-state measurements which show that the 1512-cm^{-1} species has an unprotonated Schiff base, whereas the 1466-cm^{-1} species has a protonated Schiff base.

When the correlation diagram is drawn for these data on deuterated bacteriorhodopsin using bR_{570} and M_{412} data points as standards two features emerge. First, there is an increase in slope in comparison to the protonated bacteriorhodopsin plot. This arises naturally from the $\sqrt{M}$ (M = reduced mass) dependence on the slope of such a proposed linear correlation. Furthermore, notice that the 1495-cm^{-1} C=C stretch correlates well with a λ_{max} of 460 to 480 nm, and the 1478 cm^{-1} C=C stretch correlates favorably with a λ_{max} between 525 nm and 545 nm. These predicted absorption maxima are the same to within experimental error (see Figure 12) as the corresponding predictions for native bacteriorhodopsin. Thus, the above results support not only our assignments to L_{550} and X, but also the linearity of these plots for bacteriorhodopsin and the intermediates studied in this work.

Although we are confident that the 1552-cm^{-1} band can be assigned to a new species X which arises before M_{412}, no such species has been identified by transient absorption spectroscopy on the time scale of 10–30 μs as required by our kinetic resonance Raman data. This could probably be explained by the presence of strongly overlapping absorptions and similar kinetic parameters. In this regard it is interesting to point out that a reinvestigation of the absorption data on the squid system has indicated that a previously undetected intermediate (mesorhodopsin λ_{max} = 475 nm) is present between lumirhodopsin and acid metarhodopsin (Ebina et al., 1975). Finally, it should be noted that the 1537-cm^{-1} band that can be assigned to L_{550} from the kinetic data cannot be assigned unambiguously in the steady state spectrum of bacteriorhodopsin (Figure 7A). It is possible that the N_{520} intermediate also exhibits a band in this region and, thus, may complicate the assignment of the 1537-cm^{-1} band in the steady-state spectrum.

Structural Information Concerning L_{550} and X. Structural information about L_{550} and the new species X can be obtained by examining the kinetic data found in Figures 7 and 8. Due to resonance enhancement factors, Figure 7 (457.9-nm kinetics) favors species X (λ_{max} between 460 and 480 nm), whereas Figure 8 (568.2-nm kinetics) favors L_{550}. Thus in examining species X and L_{550} we will refer to Figures 7 and 8, respectively.

By inspection of Figure 7 it appears that species X exhibits a band at 1165 cm^{-1} which does not occur in either bR_{570} or M_{412}. It is also evident that the 973, 1225, and 1619 cm^{-1} bands develop in intensity faster than the 1566 cm^{-1} intense C=C stretch of M_{412}. On this basis we assign all three of these bands which are characteristics of unprotonated Schiff bases of retinal (see Figure 6) to species X. Further support for these assignments comes from examining the resonance Raman kinetics of bacteriorhodopsin suspended in D_2O (Ehrenberg & Lewis, in preparation). Suspension in D_2O slows down the formation of M_{412} so that more of species X can be observed. Recently, Marcus & Lewis (1977) suggested that the Schiff base linkage in bacteriorhodopsin becomes unprotonated on a time scale faster than the formation of M_{412}. The kinetic data presented in Figure 7 is consistent with this observation, and there appears to be a correlation between the increase in intensity of the 1552 cm^{-1} C=C stretch of species X and the appearance of the 1619 cm^{-1} unprotonated Schiff base C=N stretch in our kinetic data. Thus our data suggest that species X has an unprotonated Schiff base.

Although X is an unprotonated Schiff base, we cannot as yet unambiguously determine the isomeric state of the chromophore in this species. However, it is interesting to point out that the new 1165-cm^{-1} band in species X is close in frequency to an intense band which occurs in 13-cis unprotonated Schiff bases of retinal, whereas no corresponding feature occurs in the all-trans models (see Figures 6B and 6C). Thus, this may indicate that thermal isomerizations are occurring in the proton pumping cycle of bacteriorhodopsin.

As far as L_{550} is concerned the kinetic data obtained with 568.2-nm excitation and 100-μs beam transit time (Figure 8E) show most clearly the spectral features of this species. This has more to do with the decrease in relative average concentration of bR_{570} and its dominant effect on the spectra than increased in concentration of L_{550} as a function of time (unpublished calcuations). Thus in the 100-μs spectrum (Figures 8E), the 1537-cm^{-1} C=C stretch of L_{550} is a well-resolved peak. When compared with the bR_{570} spectrum of Figure 8A, definite changes are noticed in the fingerprint region of Figure 8E such as a new weak band at 1235 cm^{-1} and an increase in the relative intensity of the 1187-cm^{-1} band to the 1202-cm^{-1} band. There may also be more intensity in the 1325-cm^{-1} region relative to bR_{570}. Thus we assign these new features to L_{550}. It is interesting to note that these new L_{550} features are similar in frequency to spectral details which occur in dark-adapted bacteriorhodopsin (bR_{560}) but not in bR_{570}. Since bR_{560} is known to contain 13-cis chromophores (Oesterhelt et al., 1973; Pettei et al., 1977), we can use as a first approximation the resonance Raman spectrum of this species as a guide to model the spectrum of a 13-cis protonated Schiff base in this protein environment. Thus, it seems plausible that L_{550} might also have a chromophore conformation which is close to a 13-cis protonated Schiff base. However, it should be noted that the band envelope of the C=N^+H stretch downshifts in frequency with increasing L_{550} visibility (see Figure 8A–E). This may indicate that L_{550} has a Schiff base linkage which is somewhat less protonated than bR_{570}. Therefore, we cannot exclude the possibility that changes in the resonance Raman spectra as L_{550} is produced result simply from an alteration in the state of protonation of the Schiff base.

Summary

We conclude by presenting in Figure 13 a scheme which summarizes our data on the conformational rearrangements

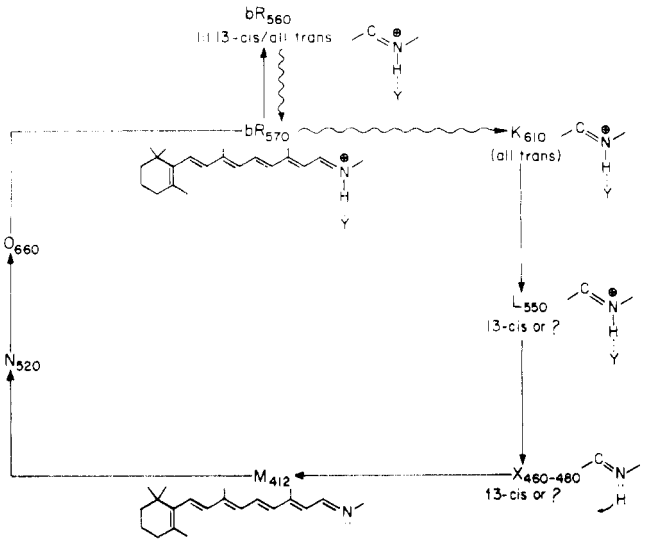

FIGURE 13: Our proposed scheme for the photochemical transformations occurring in bacteriorhodopsin's proton pumping cycle. In the protonated species, ···Y indicates interactions with one or more protein groups. The Y is not necessarily the same in each case.

which occur during bacteriorhodopsin's proton-pumping cycle. Light-adapted bacteriorhodopsin (bR_{570}) has an all-trans chromophore. At its protonated Schiff base linkage is a secondary interaction with a protein group or groups (Y). This group(s) is necessary to explain the effect on the C=N+H stretch in isotopically labeled bacteriorhodopsin. This group(s) also reconciles the observation that the chromophore in bR_{570} is not modeled accurately by a simple protonated Schiff base of butylamine.

bR_{560} apperas to also have a secondary protein–chromophore interaction at its Schiff base linkage. In addition the resonance Raman data indicate that the bR_{570} to bR_{560} thermal transition involves motion about the end of the isoprenoid chain.

K_{610} forms in about 1 ps after light absorption by bR_{570} (Kaufmann et al., 1976; Lewis et al., 1977; Ippen et al., 1978) and most likely has an all-trans chromophore which may be altered in a way that causes only slight changes in the resonance Raman spectrum. If isomerization had occurred during K_{610} formation, then we cannot understand, based on the data we have obtained on all the other species (such as relative contributions to the spectra of these species as a function of laser line, relative concentration and detection time), why no distinct spectral features are observed for K_{610}. Thus the difference in the chromophore conformation in bR_{570} and K_{610} is probably minimal. Therefore the absorption changes between bR_{570} and K_{610} may be due in part to alterations in the excited state stabilization of the chromophore by the protein as a result of light-induced protein structural alterations (Lewis, 1978).

L_{550} which forms in about 2 μs at room temperature may either have a 13-cis or ? chromophore. A new species which we call X occurs before M_{412} in the photochemical cycle. X is an unprotonated Schiff base and has an absorption maximum between 460 and 480 nm. The conformation of its chromophore is either 13-cis or ?.

M_{412} forms in about 40 μs at room temperature and also has an unprotonated Schiff base linkage. X and M_{412} lack the secondary protein–Schiff base interactions present in bR_{570}. The chromophore of M_{412} is in an all-trans conformation. At present we have no data on the return path of the cycle from M_{412} to bR_{570}.

Acknowledgments

We thank Mark van Zastrow for help in preparing the bacteriorhodopsin samples used in this investigation. We also thank Dr. Ann Lemley for obtaining resonance Raman spectra of the butylamine Schiff bases of retinal. We are indebted to Dr. H. Crespi of Argonne National Laboratories for growing fully deuterated and ^{15}N-enriched bacteriorhodopsin samples.

References

Aton, B., Doukas, A., Callender, R. H., Becher, B., & Ebrey, T. G. (1977) *Biochemistry 16,* 2995.

Becher, B., & Ebrey, T. G. (1977) *Biophys. J. 17,* 185.

Behringer, J. (1976) in *Molecular Spectroscopy* (Barrow, R. F., Long, D. A., & Millen, D. J., Eds.) Specialist Periodical Reports, Vol. 4, p 163, The Chemical Society, London.

Callender, R. H., Doukas, A., Crouch, R., & Nakanishi, K. (1976) *Biochemistry 15,* 1621.

Campion, A., El-Sayed, M., and Terner, J. (1977a) *Biophys. J. 20,* 369.

Campion, A., Terner, J., & El-Sayed, M. (1977b) *Nature (London) 265,* 659.

Chance, B., Porte, M., Hess, B., & Oesterhelt, D. (1975) *Biophys. J. 15,* 913.

Cookingham, R. E., Lewis, A., Collins, D., and Marcus, M. (1976) *J. Am. Chem. Soc. 98,* 2759.

Cookingham, R. E., Lewis, A. & Lemley, A. (1978) *Biochemistry 17* (first in a series of three papers in this issue).

Craig, N. C., & Overend, J. (1969) *J. Chem. Phys. 51,* 1127.

Danon, A., & Stoeckenius, W. (1974) *Proc. Natl. Acad. Sci. U.S.A. 71,* 1234.

Dencher, N., & Wilms, M. (1975) *Biophys. Struct. Mech. 1,* 259.

Ebina, Y., Nagasawa, N., & Tsukahara, Y. (1975) *Jpn. J. Physiol. 25,* 217.

Gill, D., Kilponen, R. G., & Rimai, L. (1970) *Nature (London) 227,* 743.

Goldschmidt, C. R., Ottolenghi, M., & Korenstein, R. (1976) *Biophys. J. 16,* 839.

Goldschmidt, C. R., Kalisky, O., Rosenfeld, T., & Ottolenghi, M. (1977) *Biophys. J. 17,* 179.

Heyde, M. E., Gill, D., Kilponen, R. G., & Rimai, L. (1971) *J. Am. Chem. Soc. 93,* 6776.

Ippen, E., Shank, C. V., Lewis, A., & Marcus, (1978) *Science 200,* 1279.

Jan, L. Y. (1975) *Vision Res. 15,* 1081.

Kalisky, O., Goldschmidt, C. R., & Ottolenghi, M. (1977) *Biophys. J. 19,* 185.

Kanner, B., & Racker, E. (1975) *Biochem. Biophys. Res. Commun. 64,* 1054.

Kaufmann, K. J., Rentzepis, P. M., Stoeckenius, W., & Lewis, A. (1976) *Biochem. Biophys. Res. Commun. 68,* 1109.

Korenstein, R., & Hess, B. (1977) *FEBS Lett. 82,* 7.

Kung, M. C., DeVault, D., Hess, B., & Oesterhelt, D. (1975) *Biophys. J. 15,* 907.

Lewis, A. (1978) *Proc. Natl. Acad. Sci. U.S.A. 75,* 549.

Lewis, A., & Spoonhower, J. (1974) in *Neutron, X-ray and Laser Spectroscopy in Biophysics and Chemistry* (Yip, S., & Chen, S., Eds.) p 347, Academic Press, New York, N.Y.

Lewis, A., Fager, R., & Abrahamson, E. W. (1973) *J. Raman Spectrosc. 1,* 465.

Lewis, A., Spoonhower, J. P., Bogomolni, R. A., Lozier, R. H.,

& Stoeckenius, W. (1974) *Proc. Natl. Acad. Sci. U.S.A. 71,* 4462.
Lewis, A., Marcus, M., Ippen, E., Shank, C. V., Hirsch, M., & Mahr, H. (1977) *Biophys. J. 17a,* 77.
Lozier, R. H., Bogomolni, R. A., & Stoeckenius, W. (1974) *Biophys. J. 15,* 955.
Marcus, M., & Lewis, A., (1977) *Science 195,* 1328.
Marcus, M. A., Lewis, A., Racker, E., & Crespi, H. (1977) *Biochem. Biophys. Res. Commun. 78,* 669.
Mathies, R., Oseroff, A., & Stryer, L. (1976) *Proc. Natl. Acad. Sci. U.S.A. 73,* 1.
Mathies, R., Freedman, T. B., & Stryer, L. (1977) *J. Mol. Biol. 109,* 367.
Mendelsohn, R. (1973) *Nature (London) 243,* 22.
Mendelsohn, R. (1976) *Biochim. Biophys. Acta 427,* 295.
Mendelsohn, R., Verma, A. L., Bernstein, H. J., & Kates, M. (1974) *Can. J. Biochem. 52,* 774.
Mitchell, P. (1961) *Nature (London) 191,* 144.
Mitchell, P. (1966) *Biol. Rev. 41,* 445.
Oesterhelt, D., & Stoeckenius, W. (1971) *Nature (London) New Biol. 233,* 149.
Oesterhelt, D., & Stoeckenius, W. (1973) *Proc. Natl. Acad. Sci. U.S.A. 70,* 2853.
Oesterhelt, D., Meentzen, M., & Schuhmann, L. (1973) *Eur. J. Biochem. 40,* 453.
Perreault, G. J., Cookingham, R. E., Spoonhower, J. P., & Lewis, A. (1976) *Appl. Spectrosc. 30,* 614.
Pettei, M. J., Yudd, A. P., Nakanishi, K., Henselmann, R., & Stoeckenius, W. (1977) *Biochemistry 16,* 1955.
Proffitt, W., & Porto, S. P. S. (1973) *J. Opt. Soc. Am. 63,* 77.
Racker, E., & Stoeckenius, W. (1974) *J. Biol. Chem. 249,* 662.
Rimai, L., Kilponen, R. G., & Gill, D. (1970) *J. am. Chem. Soc. 92,* 3824.
Rimai, L., Gill, D., & Parsons, J. L. (1971) *J. Am. Chem. Soc. 93,* 1353.
Spoonhower, J. (1976) Ph.D. Thesis, Cornell University.
Stoeckenius, W., & Lozier, R. (1974) *J. Supramol. Struct. 2,* 769.
Stoeckenius, W., Lozier, R. H., & Niederberger, W. (1977) *Biophys. Struct. Mech. 3,* 65.
Sulkes, M., Lewis, A., Lemley, A., & Cookingham, R. (1976) *Proc. Natl. Acad. Sci. U.S.A. 73,* 4266.

A Circular Dichroism Study of the Interaction of Chlorpromazine with Mouse Brain Tubulin†

A. G. Appu Rao, David L. Hare, and John R. Cann*

ABSTRACT: A circular dichroism study with subsidiary ultracentrifuge measurements on the interaction of chlorpromazine with mouse brain tubulin establishes the previous inference from binding studies that the drug induces a change in the structure of the protein. Binding of the first mole of chlorpromazine causes an alteration in secondary structure, which is reversible with respect to drug concentration, without detected change in tertiary structure or significant change in the state of association of the protein. The conformationally altered tubulin binds additional chlorpromazine molecules without further change in secondary structure.

The tranquilizing drug chlorpromazine hydrochloride [2-chloro-10-(*N,N*-dimethylaminopropyl)phenothiazine hydrochloride] interacts reversibly in vitro with mouse brain microtubule subunit protein, tubulin, as revealed by inhibition of the rate of reassembly of microtubules and the binding of colchicine (Cann and Hinman, 1975), and by direct binding measurements (Hinman and Cann, 1976). Chlorpromazine binds reversibly to tubulin via two well-resolved processes: One CPZ[1] molecule binds strongly compared to eight to nine molecules which bind weakly and with moderately weak cooperativity (Hill constant of 2.8). This behavior implies a macromolecular structural change, which is substantiated in the study described below.

Materials and Methods

Preparation of Tubulin. Purified tubulin was prepared by DEAE-cellulose chromatography (Eipper, 1972). The excised brains of 15–18 adult mice (Texas Inbred, ICR) were homogenized manually in 2.5 volumes of PMS buffer. The homogenate was centrifuged at 100 000*g* for 60 min, and the supernatant was applied to a column of DEAE-cellulose (bed volume, 1.5 × 26 cm) which had been equilibrated with PMS buffer plus 0.15 M NaCl. After eluting the column with PMS buffer plus 0.15 M NaCl to remove extraneous proteins, the tubulin was eluted with PMS buffer plus 0.3 M NaCl. The center fractions from the tubulin peak were pooled, and solid sucrose was dissolved in the sample to give a final concentration of 1 M when required. All of these operations were carried out at 0–4 °C, and the resulting stock solution of tubulin was maintained in an ice bath for the rest of the day's experimentation.

The purity of the tubulin thus prepared was established by

† From the Department of Biophysics and Genetics, University of Colorado Medical Center, Denver, Colorado 80262. *Received May 5, 1978.* Publication no. 721. Supported in part by Research Grant 5 R01 HL13909-26 from the National Heart, Lung, and Blood Institute and by National Institute of General Medical Sciences Training Grant 5 T01 GM00781, National Institutes of Health, United States Public Health Service.

[1] Abbreviations used are: CPZ, chlorpromazine; DEAE, diethylaminoethyl; PMS buffer, 0.05 M sodium pyrophosphate, 2.5 × 10^{-3} M $MgCl_2$, 7.3 × 10^{-3} M sucrose, adjusted to pH 6.8 with HCl; PMHS buffer, same as PMS buffer except that the sucrose concentration is 1 M; $NaDodSO_4$, sodium dodecyl sulfate; CD, circular dichroism.

0006-2960/78/0417-4735$01.00/0